doi: 10.3304/JMES.2019.003

Journal of Mediterranean Earth Sciences 11 (2019), 31-45

Journal of Mediterranean Earth Sciences

P-T estimates from amphibole and plagioclase pairs in metadolerite dykes of the Frido unit (southern Apennines-Italy) during the ocean-floor metamorphism

Giovanna Rizzo [1,*], Filomena Canora [2], Maria Carmela Dichicco [1], Salvatore Laurita [1], Maria Teresa Cristi Sansone [1]

[1] *Dipartimento di Scienze, Università della Basilicata, Campus di Macchia Romana Potenza, Italy*
[2] *Scuola di Ingegneria, Università della Basilicata, Campus di Macchia Romana, Potenza, Italy*
[*] *Corresponding author: giovanna.rizzo@unibas.it*

ABSTRACT - The metadolerite dykes from the Frido ophiolitic sequence of the Pollino Massif (southern Apennines, Italy) reflect strain partitioning with textures evolving from magmatic intersertal/intergranular, blast-ophitic to incomplete metamorphic recrystallization.

Amphibole and plagioclase are the main constituent minerals in these rocks. Amphibole composition reflects both bulk compositional and P-T changes. Different Ti and IVAl values between the brown and green amphiboles clearly indicate genetic conditions of amphiboles developed in ocean-floor hydrothermal metamorphic conditions.

The electron microprobe analysis showed that, the assemblage developed during ocean-floor hydrothermal type metamorphism (M1) consists of two main amphibole varieties: a brown and a green one; instead, a blue amphibole developed during orogenic metamorphism (M2).

The magmatic plagioclase is anorthite (PL1) whereas the metamorphic plagioclases are oligoclase (PL2) and albite (PL3). The estimated P-T conditions support the idea of under ocean-floor hydrothermal metamorphism. The variety of amphibole compositions and the plagioclase found in the metadolerite dykes offers useful constraints to reconstruct of the related environmental conditions, providing new insights on the oceanic metamorphic evolution of this orogenic sector of southern Apennines.

Keywords: amphibole; plagioclase; metadolerite dykes; ophiolitic sequences, ocean-floor hydrothermal metamorphism; Frido Unit; Liguride accretionary wedge; southern Apennines.

Submitted: 11 December 2018-Accepted: 10 April 2019

1. INTRODUCTION

Metadolerites can be found in many ophiolitic sequences. In the southern Apennines, the Liguride accretionary wedge includes ophiolitic slices that mostly consist of serpentinites crosscut by metadolerite dykes. The metadolerite dykes cut through serpentinized peridotites and are affected by rodingitic alterations and ocean-floor metamorphism (Sansone et al., 2011). The presences of these dykes is typical of slow-spreading mid-ocean ridges (Sansone et al., 2011). These rocks show a metasomatic and a polyphase metamorphic evolution correlated with both the ocean-floor metamorphism and their emplacement within the Liguride accretionary wedge (Sansone et al., 2011). Mineral assemblages of ocean-floor metamorphism are typical of amphibolite and greenschist facies (Sansone et al., 2011). The subsequent subduction related metamorphism under relatively high pressure and low temperature (blueschist facies) conditions affected the rocks during the formation of the Apennine accretionary wedge (Sansone et al., 2011).

During their metamorphic evolution, metadolerite dykes recorded two main events: i) the M1 event under greenschist to amphibolite facies conditions, testified by the occurrence of oceanic Ca-amphiboles; and ii) the subsequent M2 event (orogenic metamorphism) developed under HP/LT blueschist facies metamorphism linked with the Alpine event as testified by the occurrence of Ca-Na-amphibole and interpreted as the initial stage of the orogenic phase overprinted by an orogenic-type Na-amphibole (Laurita and Rizzo, 2018).

Within the assemblage of ocean-floor metamorphism, brown- green- blue/green- and pale green/colorless-amphiboles are found dispersed throughout the metadoleritic matrix. Metadolerite dykes crosscutting serpentinite rocks (Sansone and Rizzo, 2009; Sansone et al., 2011) show MORB-type affinity (Sansone et al., 2011) and are comparable to the oceanic crust domains observed in the central Atlantic (Bonatti, 1968; Miyashiro et al., 1969; Aumento and Loubat, 1971; Bonatti, 1976; Lagabrielle and Cannat, 1990; Mével et al., 1991; Cannat et al., 1997), where gabbros and serpentinized upper-mantle rocks form a significant part of the sea floor along the active axis (Lagabrielle and Cannat, 1990). The western Tethys is analogous to the slow-spreading oceans, like the Atlantic Ocean (Lemoine et al., 1987; Lagabrielle and Cannat, 1990; Cannat, 1996; Cannat et al., 1997; Magde et al., 2000; Rabain et al., 2001). The compositions of amphibole-plagioclase pairs are a monitor of the polyphase metamorphic evolution affecting those rocks: i.e. an early ocean-floor metamorphism and an HP/LT metamorphic overprint related to subduction testified by the occurrence of glaucophane, Mg-riebeckite, lawsonite, pumpellyite, phengite and aegirin-augite (Sansone et al., 2011; Sansone and Rizzo, 2012; Sansone et al., 2012 a,b). Metadolerites contain amphiboles of various chemical compositions (Ca-, Ca-Na-, and Na-amphiboles). However, in previous studies of the Frido Unit metadolerites did not undertake any detailed investigation of hydrous phases. In order to better constrain the metamorphic evolution of the Frido Unit metadolerite dykes of the Liguride accretionary wedge (southern Apennines), we provide, in this work, new petrographic and geochemical data of amphibole and plagioclase pairs obtained by optical microscopy and electron-probe micro analysis (EMPA) to testify that these rocks have been affected by ocean-floor metamorphism under amphibolite to greenschists facies conditions.

2. GEOLOGY OF THE STUDY AREA

The study area is located in the southern Apennines chain, developed between the Upper Oligocene and the Quaternary as a result of the convergence between the African and European plates (Gueguen et al., 1998; Cello and Mazzoli, 1999; Doglioni et al., 1999; Scrocca, 2010). In the southern Apennines at the Calabria-Lucanian border zone ophiolitic slices are part of the Liguride accretionary wedge (Fig. 1a) and have been attributed to the Jurassic Tethyan ocean by many authors (Vezzani, 1970; Amodio Morelli et al., 1976; Spadea, 1976, 1982, 1994; Lanzafame et al., 1979; Knott, 1987, 1994; Tortorici et al., 2009; Cirrincione et al., 2015).

The Liguride accretionary wedge has been interpreted as the suture zone between the converging paleo-Europe and paleo-African plates and consists from bottom to top, of the Frido Unit, the Episcopia-San Severino Mélange, the Northern Calabrian Unit, and the Sicilian-type terranes (Knott, 1987, 1994; Bonardi et al., 1988; Monaco et al., 1991; Tortorici et al., 2009; Barca et al., 2010; Dichicco et al., 2015).

The Frido Unit ophiolites consist of cataclastic serpentinites (Dichicco et al., 2015, 2017, 2018, 2019), metagabbros, metabasalts and diabases and continental crust rocks (Laurita et al., 2014; Rizzo et al., 2016), covered by a metasedimentary sequence (Vezzani, 1970; Spadea, 1982, 1994; Rizzo et al., 2016) as observed in the area of Timpa delle Murge (southern Apennines). The presence of both oceanic and continental crust rocks, as well as a portion of upper mantle suggest that the Frido Unit originated in an ocean-continent transition (OCT) domain (Vitale et al., 2013; Laurita and Rizzo, 2018). Instead, some authors (Spadea, 1982; Bonardi et al., 1988) interpret the coupling between the ultramafic rocks and rocks with continental crust affinity as a mélange reflecting the presence of the tectonic contact.

Some of the rocks belonging to the Frido Unit are characterized by a blueschist facies metamorphism (Spadea, 1982, 1994; Monaco et al., 1995; Vitale et al., 2013) According to some authors (Laurita and Rizzo, 2018) blueschist facies metamorphism in mafic rocks developed at peak pressure conditions of 8-12 kbar and temperature values of 300-400 °C.

3. ANALYTICAL METHODS

Selected samples of metadolerite dykes (Figs. 1b, 2) of the Frido Unit were collected at the Timpa della Guardia close to the San Severino Lucano village (Fig. 1a; Tab. 1). Petrographic characterization of all the samples was carried out by optical microscopy, using a ZEISS polarizing microscope, on thin sections of rock samples.

The chemical characterization was performed using a X-ray fluorescence (XRF BRUKER S8-TIGER) at the Department of Biology, Ecology and Earth Sciences (DiBEST), University of Calabria (Arcavacata di Rende, Cosenza, Italy). Each samples was cleaned for geochemical analyses. Weathered coats and veined surfaces were cut off. Elemental analyses for major (wt%: SiO_2, TiO_2, Al_2O_3, Fe_2O_3, MnO, MgO, CaO, Na_2O, K_2O, and P_2O_5) and some trace elements (ppm: Ni, Cr, V, Ce, Co, Ba, Nb, Y, Sr, Zr, S, Cl, Cu, Zn, Rb, Sn and Pb) concentrations were obtained. The XRF analysis was performed on pressed powder pellets of whole-rock samples (prepared by milling to a fine-grained powder in an agate mill) and compared to international standard rock analyses (AGV-1, AGV-2, BCR-1, BCR-2, BR, DR-N, GA, GSP-1, GSP-2 and NIM-G) of the United States Geological Survey. The estimated precision and accuracy for trace elements are better than 5%, except for those elements having a concentration of 10 ppm or less (10-15%). Total Loss On Ignition (L.O.I.) was determined after heating the samples for 3 h at 900 °C.

The whole rock chemical composition by XRF was used for the calculation of the P-T pseudo-sections. Computations have been done using Theriak/Domino software. Pseudo-sections were calculated using the database by Berman (1988). For the mineral assemblages and compositions mentioned above, the NCKMFASH (Na_2O, CaO, K_2O, FeO, MgO, Al_2O_3, SiO_2, H_2O) model system was selected for one representative sample (MC77) to calculate pseudo-sections. Fluid phase is assumed to be pure H_2O and considered to be in excess, because the

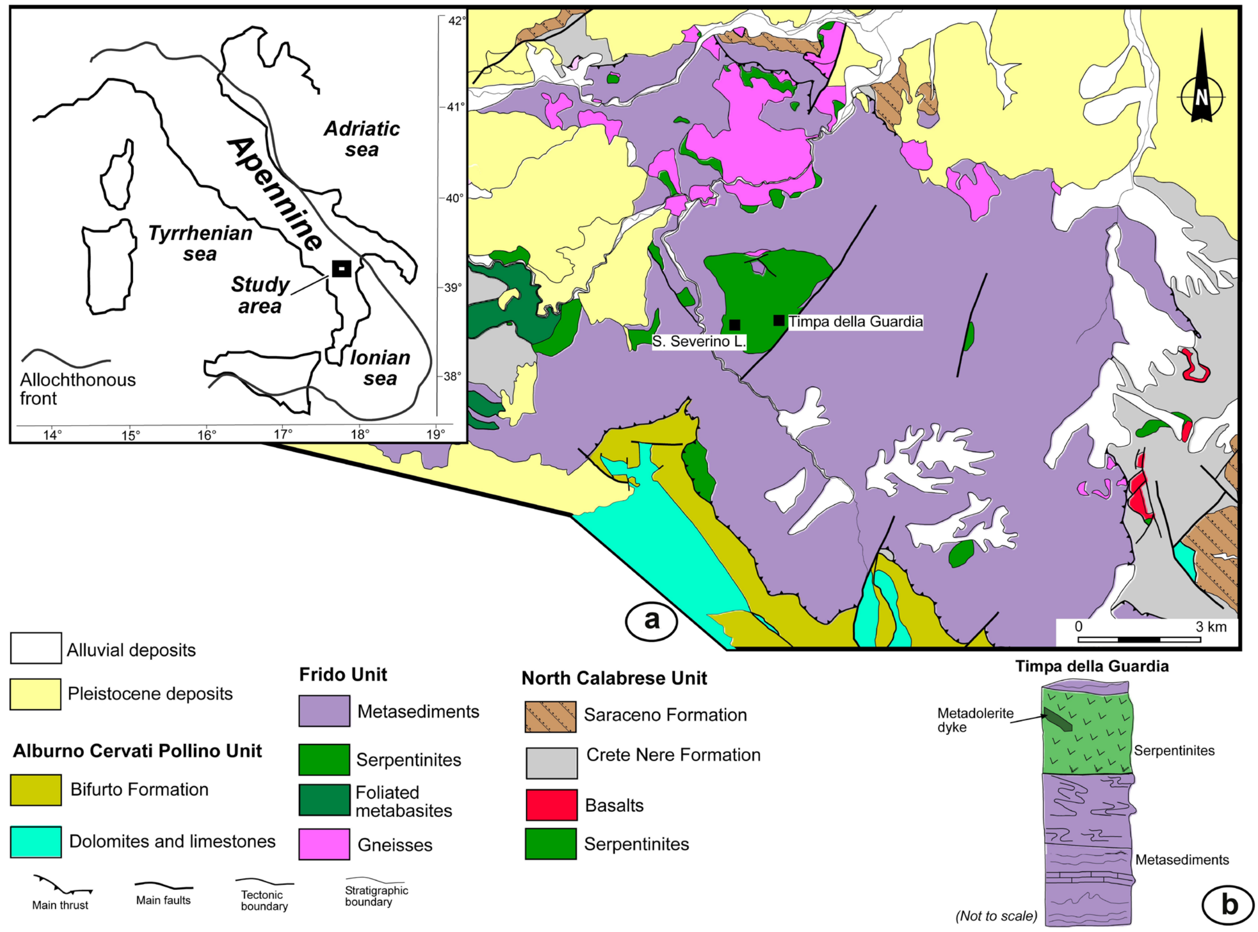

Fig. 1 - a) Geographic location of the study area and simplified geological sketch map; b) Tectono-stratigraphic column.

Fig. 2 - Example of outcrops of metadolerite dykes at Timpa della Guardia locality (southern Apennines, Italy).

hydrous phases as Amph, Chl, Ep, Lws occur in all of metamorphic stages in metadolerite dykes.

Electron probe micro analyses were performed on amphibole and plagioclase using a JEOL JXA-8200 probe, equipped with five WDS spectrometers and an EDS spectrometer, at the Dipartimento di Scienze della Terra "Ardito Desio" of the University of Milan. The analytical conditions were: 15 kV accelerating voltage and 15 nA beam current; count time 30 s at peak and 10 s at background. Natural oxides were used as standards.

Symbols for minerals in the text, tables are those recommended by Siivola and Schmid (2007) and Whitney and Bernard (2010). The exceptions are indicated by the following symbols: br Am* (brown amphibole) gr Am*

Tab. 1 - Petrographic features of the Frido Unit metadolerite dykes.

Sample	*Texture*	*Metamorphic minerals*	*Sampling localities**
MC2	Mylonitic	Chl+p/c Am*+Pmp+Qtz+Prh+wht Mc*	TDG
MC14	Blasto-ophitic	Chl+gr Am*+Pmp+Qtz+Prh+wht Mc*	RVF-SSL (km 45)
MC18	Blasto-ophitic	Chl+gr Am*+Pmp+Qtz+Prh+wht Mc*	RVF-SSL (km 46)
MC20	Blasto-ophitic	Chl+p/c Am*+Pmp+Qtz+Prh+wht Mc*	TDG
MC35	Intersertal/intergranular	Chl+gr Am*+Pmp+Qtz+Prh+wht Mc*	TDG
MC49	Blasto-ophitic	Chl+gr Am*+Pmp+Qtz+Prh+wht Mc*	TDG
MC74	Blasto-ophitic	Chl+gr Am*+Pmp+Qtz+Prh+wht Mc*	TDG
MC3	Blasto-ophitic	br Am*+Chl+Pmp+wht Mc*+Qtz+Prh+p/c Am*+gr Am*	TDG
MC6	Blasto-ophitic	br Am*+Chl+Pmp +wht Mc*+ Qtz+Prh+gr Am*+p/c Am*	TDG
MC23	Blasto-ophitic	br Am*+Chl+Pmp+wht Mc*+Qtz+Prh+p/c Am*	TDG
MC29	Intersertal/intergranular	br Am*+Chl+Pmp+wht Mc*+Qtz+Prh+gr Am*	TDG
MC32a	Intersertal/intergranular	br Am*+Chl+Pmp+wht Mc*+Qtz+Prh+gr Am*	TDG
MC38	Intersertal/intergranular	br Am*+Chl+gr Am*+Pmp+Qtz+Prh+wht Mc*	TDG
MC42	Blasto-ophitic	br Am*+Chl+Pmp+wht Mc*+Qtz+Prh+gr Am*	TDG
MC45	Blasto-ophitic	br Am* +Chl +Pmp+wht Mc*+Qtz +Prh+gr Am*	TDG
MC51	Blasto-ophitic	br Am*+Chl+Pmp+wht Mc*+Qtz+Prh+gr Am*	TDG
MC65	Blasto-ophitic	br Am*+Chl +Pmp+wht Mc*+Qtz+Prh+gr Am*+p/c Am*	CTC
MC68	Intersertal/intergranular	br Am*+Chl+Pmp+wht Mc*+Qtz +Prh+gr Am*	FB
MC71	Blasto-ophitic	br Am*+Chl+Pmp+wht Mc*+Qtz+Prh+gr Am*	TDG
MC72	Mylonitic	br Am*+Chl+Pmp+wht Mc*+Qtz+Prh+gr Am*	TDG
MC73	Blasto-ophitic	br Am*+Chl+Pmp+wht Mc*+Qtz+Prh+p/c Am*	TDG
MC75	Blasto-ophitic -mylonitic	br Am*+Chl+Pmp+wht Mc*+Qtz+Prh+p/c Am*	TDG
MC76	Blasto-ophitic	br Am*+Chl+Pmp+wht Mc*+Qtz+Prh+gr Am*	TDG
MC40	Blasto-ophitic	Ab(Pl_3)+Olg*(Pl_2)+br Am*+Qtz+Chl+gr Am*+p/c Am*+bl Am*+Lws+wht Mc*+Prh	TDG
MC69	Intersertal/intergranular	Ab(Pl_3)+Olg* (Pl_2)+br Am*+gr Am*+p/c Am*+Qtz+Chl+bl Am*+Lws+wht Mc*+Prh	TG
MC70	Blasto-ophitic	Ab (Pl_3)+Olg* (Pl_2)+Cpx+br Am*+gr Am*+p/c Am*+gr/bl Am*+Qtz+Chl+bl Am*+Lws+wht Mc*+Prh	FA; RVF-SSL to the km 45
MC77	Blasto-ophitic	Ab(Pl_3)+Olg* (Pl_2)+Cpx+br Am*+gr Am*+p/c Am*+Qtz+Chl+bl Am*+Lws+wht Mc*+Prh	PM
MC81	Blasto-ophitic	br Am*+gr Am*+p/c Am*+bl/gr Am*+Olg*(Pl_2)+Ab (Pl_3)+Qtz+Chl+bl Am* +Lws+wht Mc*+Prh	FA

* Timpa della Guardia (TDG); Cava di Timpa Castello (CTC); Fosso Arcangelo (FA); Piani Matteo (PM); Fosso di Ballarano (FB); Manca di Sopra (MS); Timpa della Gatta (TG); Road Valle Frida –San Severino Lucano (RVF-SSL); Fosso Arcangelo (FA).

(green amphiboles), p/c Am* (pale-green/colourless amphiboles), bl/gr Am* (blue-green amphiboles), bl Am* (blue amphiboles), Olg*(oligoclase).

4. METADOLERITE DYKES

4.1. PETROGRAPHY

Metadolerites characteristically display prominent strain partitioning with well preserved domains showing primary intersertal or intergranular (Fig. 3a), relicts of ophitic texture (blasto-ophitic texture) (Fig. 3b) and highly deformed zones with mylonitic textures (Fig. 3c) (Sansone et al., 2011; Sansone et al., 2012 a,b). Amphibole and plagioclase are the main minerals in the metadolerite dykes. Amphiboles are associated with magmatic plagioclase (PL1), clinopyroxene (augite and augite-diopside compositions, Sansone and Rizzo, 2012) and opaque minerals; these were identified as primary magmatic minerals. The magmatic minerals were re-equilibrated under near magmatic subsolidus conditions, as testified by the polygonal texture of clinopyroxene and plagioclase (Fig. 4).

As far as secondary minerals, some primary crystals show sericite or saussurite alteration, while others were

Fig. 3 - Photomicrographs of various textures of metadolerite dykes: a) Intersertal texture; Plane-polarized light; 4X. Scale bar = 250 µm. b) Blastophitic texure; Plane-polarized light; 4X. Scale bar = 150 µm. c) Mylonitic fabric and veins cutting metadolerites; Plane-polarized light; 4X. Scale bar = 200 µm.

replaced by fine-grained aggregates of pumpellyite, prehnite, chlorite, and epidote. The magmatic clinopyroxene is augite. It was replaced by chlorite, white mica, and various types of amphibole; some individuals show twinning and are often zoned, sometimes showing undulose extinction. Clinopyroxene shows an overgrowth of opaque minerals such as titanite, Fe-hydroxides, epidote, and apatite. Metamorphic mineral assemblages are: chlorite, quartz, epidote, albite (PL3), prehnite, pumpellyite, phengite (Sansone and Rizzo, 2012), titanite, apatite, blue-amphibole and lawsonite (Tab. 1). Polymineral veins cross-cut metadolerites (pumpellyite, chlorite, prehnite, albite (PL3), tremolite/actinolite, white mica, quartz, calcite, albite, epidote, lawsonite, glaucophane, and chrysotile) (Sansone et al., 2011; Sansone and Rizzo, 2012). Brown amphibole occurred as neoblasts, or as coronas rimming clinopyroxene (Fig. 5c). Amphibole is pleochroic from yellow to brown color. Extinction angle (c/γ) is typically in the range between 15° and 20°, and 2V is 70°. Some crystals are pseudomorphs after clinopyroxene, are twinned and show exsolution lamellae of rutile (Fig. 5 a,b). Opaque minerals and apatite occur as inclusions.

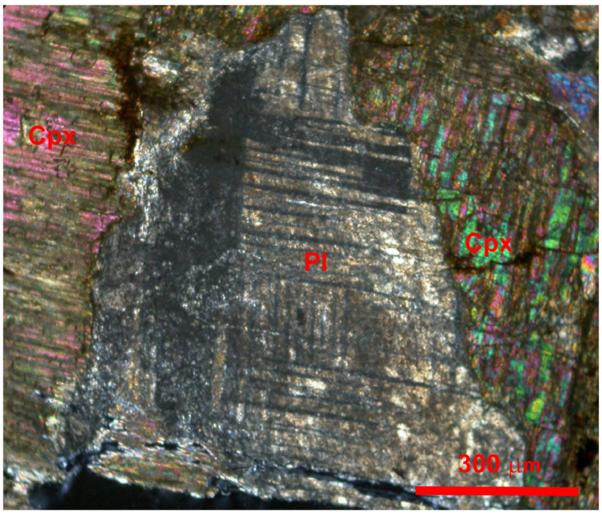

Fig. 4 - Photomicrographs of polygonal texture of clinopyroxene and plagioclase. Plane-polarized light. Scale bar = 300 µm.

Green amphibole occurs as neoblasts forming coronas rimming brown amphibole or clinopyroxene (Fig. 5c). Pleochroism varies from yellow-green to green colour. Extinction angle (c/γ) is comprised between 26° and 33°, and optical sign is negative and 2V is 60°.

Neoblasts of pale-green amphibole, which are actinolitic in composition, are pseudomorphs after clinopyroxene and occur in the veins. Pleochroism varies from colorless to pale green color. Extinction angle (c/γ) is comprised between 25° and 27°, and optical sign is negative and 2V is 70°. The pale-green amphibole in the veins sometimes shows ductile deformation.

Blue-green amphibole occurs either as single crystals or around pale green/colorless amphiboles (Fig. 6a). Light blue amphibole, glaucophane or magnesio-riebeckite in composition (c/γ 20°) (Sansone et al., 2012 a,b) commonly rims the brown and pale green amphibole grains (Fig. 6b). The optical sign is negative with 2V small.

4.2. BULK CHEMISTRY

Whole-rock chemical analyses for major elements (SiO_2, TiO_2, Al_2O_3, Fe_2O_3, MnO, MgO, CaO, Na_2O and P_2O_5) expressed as wt% in the metadolerite dykes are reported in Appendix I. Major element data show that SiO_2 is between 41.5 to 45.8 wt%, followed by Al_2O_3 (13.39 to 17 wt%), Fe_2O_3 (9.3 to 11.1 wt%) and CaO (8.0 to 15.2 wt%) and MgO (9.07 to 14.52 wt%). Results show a low concentrations in MnO (0.14 to 0.20 wt%), Na_2O (0.39 to 3.30 wt%), P_2O_5 (0.05 to 0.25 wt%).

4.3. CHEMISTRY OF AMPHIBOLES

The amphibole compositions (Tab. 2, Appendix II) are obtained using the Amphibole Classification Excel Spreadsheet 2013 proposed by Locock (2014). This spreadsheet classifies amphibole chemical analyses into group, subgroup, and species. It follows the set of recommendations approved by the Commission on New Minerals Nomenclature and Classification (CNMNC) of the International Mineralogical Association (IMA) which was published by Hawthorne et al. (2012)=IMA 2012. The output includes the normalization procedures that

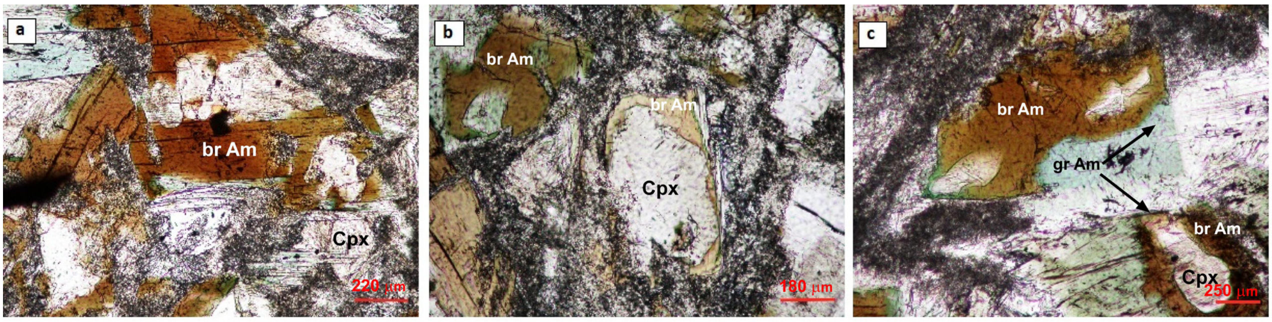

Fig. 5 - Photomicrographs: a) Brown amphibole pseudomorphs after clinopyroxene; Plane-polarized light. Scale bar = 220 µm. b) Brown amphibole coronas rimming clinopyroxene; Plane-polarized light. Scale bar = 180 µm. c) Green amphibole crystallized forming corona rimming brown amphibole or clinopyroxene; Plane-polarized light. Scale bar = 250 µm.

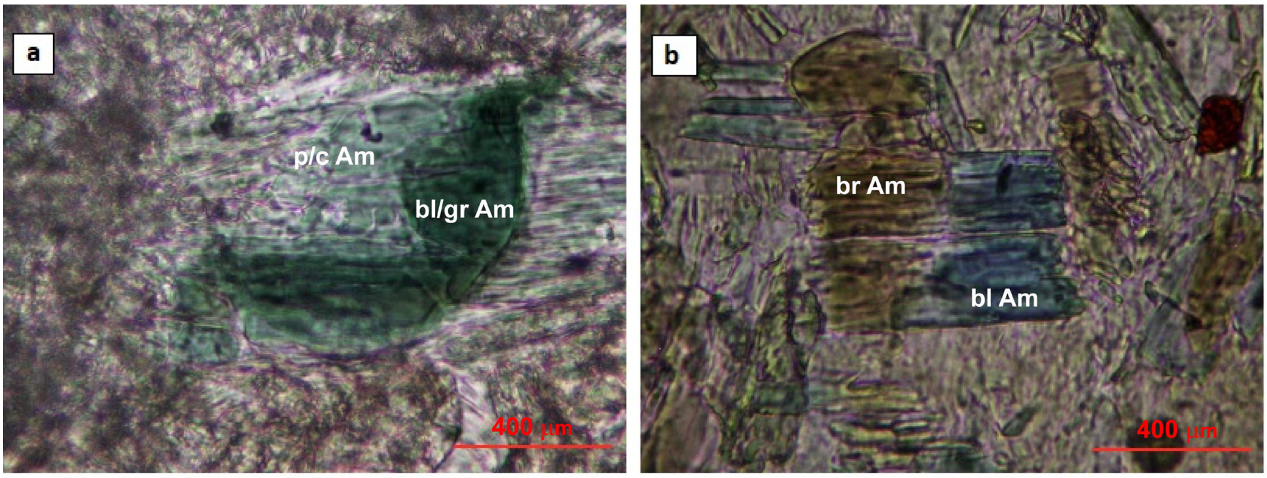

Fig. 6 - Photomicrographs: a) Blue-green amphibole and rim of pale green/colorless amphiboles; Plane-polarized light. Scale bar = 400 µm. b) Blue amphibole rims developed after the brown amphibole; Plane-polarized light. Scale bar = 400 µm.

were used. For those analyses where the initial values for the valence states of Fe and Mn were retained throughout the algorithm, the result "per 24 (O, OH, F, Cl)" is given instead (Locock, 2014). For each analysis, the values used in the final formula proportions of the ratios Fe^{3+}/ΣFe and Mn^{3+}/ΣMn are given, along with the final values in weight percent of MnO, Mn_2O_3, FeO, Fe_2O_3, H_2O^+ and the final total of the weight percent data (Locock, 2014) and nomenclature of amphiboles conforms to the recommendations of Hawthorne et al. (2012).

The analyzed amphiboles show brown, green, pale green/colourless, blue, and blue-green colour at plane-polarized light. They include calcium amphiboles (Fig. 7), sodium-calcium-amphiboles and sodium amphiboles (Sansone et al., 2012 a,b).

Amphiboles show a nearly continuous range from high-Al pargasitic to low-Al actinolitic compositions (Fig. 7). Brown amphiboles with similar compositional variations are also observed in gabbroic rocks at other slow-spreading ridge locations (Mével, 1987, 1988). The brown amphibole individuals are pargasite, Ti-rich pargasite, Mg-hastingsite, Ti-rich Fe sadanagaite, Ti-Fe tschermakite, Fe-rich barroisite. Differences in Ti and ^{IV}Al values (Fig. 8) between the brown and green amphiboles clearly indicate different genetic conditions during ocean-floor metamorphism. The brown amphiboles are indicative of genesis at a higher temperature than the green amphiboles (Raase, 1974; Robinson et al., 1982; Mével and Cannat, 1991), and the lower Ti: ^{IV}Al ratio in the green amphiboles than in the amphiboles from other oceanic environments suggest a lower geothermal gradient (P-T estimates yield temperatures ranging from 660° to 880° C at very low pressure) (Puga et al., 2002). The trend of increasing temperature for the ocean floor amphiboles is probably due to their chemical variations and, as a result, the rocks are hydrated by metamorphic recrystallization, resulting in an increasingly limited supply of seawater, as deduced by Vanko (1986) and Stakes and Vanko (1986) for amphiboles of the Mathematician Ridge (Puga et al., 2002). The high TiO_2 contents and the moderate K_2O contents in the brown amphibole are compatible with the amphiboles that originated from ocean-floor metamorphism along ridges (Mével, 1987; Gillis et al., 1993) and in ophiolites (Cortesogno and Lucchetti, 1984). Green amphibole compositions range from Fe-tschermakite, Fe-sadanagaite, Mg-Fe-hornblende to tremolite-actinolite. Pale-green/colorless amphibole shows actinolite and pargasite compositions, the blue-green amphiboles has Fe-tschermakite and pargasite compositions, while blue amphibole (Mg-riebeckite).

Tab. 2 - Representative chemical analyses of amphibole (values in wt%). N.d. = Not detected

Sample	MC81	MC81	MC81	MC81	MC81	MC77	MC77	MC77	MC77	MC77	MC77
N. Analysis	203	204	216	205	217	77	69	70	75	116	117
Occurences	br Am* after Cpx	br Am* after Cpx	br Am* after Cpx	p/c Am*	p/c Am*	p/c Am*	br Am*	br Am* after Cpx	br Am*	bl/gr Am*	bl/gr Am*
Oxides (wt%)											
SiO_2	44.72	48.57	44.61	55.19	54.92	44.84	43.16	46.67	45.00	43.55	42.30
TiO_2	1.54	1.24	2.77	0.06	0.05	0.18	0.16	0.40	0.08	0.09	0.12
Al_2O_3	11.10	7.8	9.74	0.53	0.72	11.69	13.42	9.40	11.59	14.46	14.74
Cr_2O_3	n.d.	0.04	0.03	0.02	n.d.	n.d.	n.d.	n.d.	n.d.	0.02	n.d.
FeO	12.86	11.44	13.16	17.47	16.60	15.36	14.91	13.77	15.94	13.85	14.85
MnO	0.26	0.30	0.24	0.20	0.17	0.26	0.22	0.25	0.29	0.19	0.29
MgO	14.07	16.16	13.60	13.18	13.56	13.11	12.53	14.94	12.99	12.66	12.46
CaO	10.93	10.77	10.90	12.28	11.98	10.62	10.91	10.70	10.33	11.29	10.93
Na_2O	3.16	2.52	3.19	0.30	0.50	2.80	3.10	2.48	2.80	3.12	3.25
K_2O	0.28	0.23	0.37	0.04	0.05	0.26	0.27	0.25	0.21	0.31	0.28
Total	98.92	99.07	98.61	99.27	98.55	99.12	98.68	98.86	99.23	99.54	99.22
Group	OH,F,Cl	OH,F,Cl	OH,F,Cl	OH,F,Cl	OH,F,Cl	OH,F,Cl	OH,F,Cl	OH,F,Cl	OH,F,Cl	OH,F,Cl	OH,F,Cl
Subgroup of (OH,F,Cl)	Ca	Ca	Ca	Ca	Ca	Ca	Ca	Ca	Ca	Ca	Ca
Species	Pargasite	Mg-hastingsite	Ti-rich pargasite	Actinolite	Actinolite	Pargasite	Pargasite	Mg-hastingsite	Pargasite	Pargasite	Pargasite
Si	6.464	6.901	6.509	7.962	7.944	6.492	6.272	6.677	6.509	6.273	6.110
$Al^{(iv)}$	1.536	1.099	1.491	0.038	0.056	1.508	1.728	1.323	1.491	1.727	1.890
T subtotal	8.000	8.000	8.000	8.000	8.000	8.000	8.000	8.000	8.000	8.000	8.000
$Al^{(vi)}$	0.355	0.207	0.184	0.052	0.067	0.486	0.570	0.262	0.484	0.728	0.619
Ti	0.167	0.133	0.304	0.007	0.005	0.020	0.017	0.043	0.009	0.010	0.013
Cr	0.000	0.004	0.003	0.002	0.000	0.000	0.000	0.000	0.000	0.002	0.000
Fe^{3+}	0.244	0.282	0.148	0.029	0.066	0.399	0.519	0.622	0.450	0.262	0.610
Fe^{2+}	1.202	0.951	1.403	2.076	1.938	1.265	1.179	0.886	1.257	1.279	1.075
Mg	3.032	3.423	2.958	2.834	2.924	2.830	2.714	3.186	2.801	2.719	2.683
C subtotal	5.000	5.000	5.000	5.000	5.000	5.000	4.999	4.999	5.001	5.000	5.000
Mn^{2+}	0.032	0.036	0.030	0.024	0.021	0.032	0.027	0.030	0.036	0.023	0.035
Fe^{2+}	0.108	0.126	0.055	0.003	0.004	0.195	0.114	0.139	0.222	0.127	0.109
Ca	1.693	1.640	1.704	1.898	1.857	1.647	1.699	1.640	1.601	1.743	1.692
Na	0.167	0.198	0.212	0.075	0.119	0.125	0.160	0.190	0.142	0.107	0.164
B subtotal	2.000	2.000	2.001	2.000	2.001	1.999	2.000	1.999	2.001	2.000	2.000
Na	0.718	0.496	0.691	0.009	0.022	0.661	0.714	0.497	0.643	0.765	0.747
K	0.052	0.042	0.069	0.007	0.009	0.048	0.050	0.046	0.039	0.057	0.052
A subtotal	0.770	0.538	0.760	0.016	0.031	0.709	0.764	0.543	0.682	0.822	0.799
Sum T,C,B,A	15.770	15.538	15.761	15.016	15.032	15.708	15.763	15.541	15.684	15.822	15.799

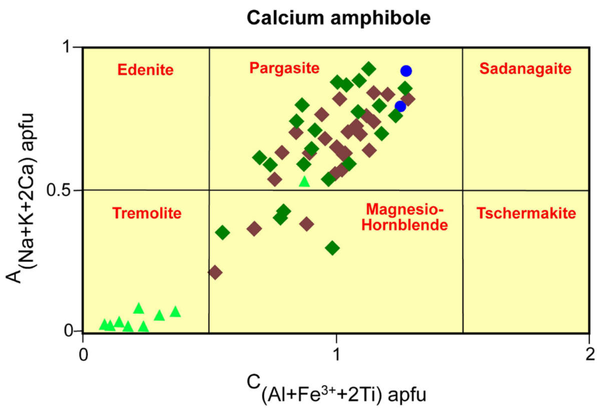

Fig. 7 - Chemical composition of Ca-amphiboles according to the nomenclature of Locock (2014). Legend: brown rhombus = brown amphibole; green rhombus = green amphibole; green triangle = pale green/colourless amphibole; blue octagon = blue amphibole.

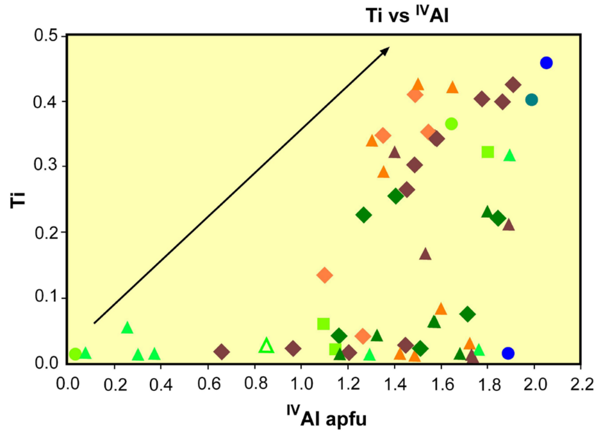

Fig. 8 - Ti vs ivAl plot of amphibole types. The arrow shows the positive correlation between Ti and Al. Legend brown amphibole: brown rhombus = Ti-rich pargasite; brown triangle = pargasite; orange triangle = Ti-rich Mg-hastingsite; orange rhombus = Mg-hastingsite. Legend blue amphibole: blue octagon = blue/green pargasite. Legend green amphibole: green square = Mg-horneblende; green octagon = green hastingsite; clear green triangle = actinolite; clear green octagon = Mg-Fe horneblende, empty triangle = Fe-pargasite; green rhombus = Mg-hastingsite; green triangle = pargasite; empty octagon = Fe-horneblende.

4.4. CHEMISTRY OF PLAGIOCLASES

The end-members of feldspars are: An, Ab and Or (anorthite, albite, and orthoclase). To determine the plagioclase mineral groups in metadolerites chemical composition of the analysed plagioclases have been plotted on Ab-An-Or diagram (Fig. 9). Table 3 and Appendix III show the plagioclase compositions based on the results of electron microprobe analysis, the number of cations is recalculated on the basis of 8 oxygens. The plagioclase grains have compositions of An>Olig>Ab, with some very minor amounts of orthoclase (see Appendix III).

4.5. CHEMISTRY OF CLINOPYROXENES

Structural formula of clinopyroxenes was calculated on the basis of 6 oxygen and classified by using the pyroxene nomenclature suggested by Morimoto (1988, 1989) the chemical composition of clinopyroxene are reported in table 4. The end-members are: Wo ($Ca_2Si_2O_6$), En ($Mg_2Si_2O_6$), Fs ($Fe_2Si_2O_6$) and Aeg ($Na_2Fe^{3+}[Si_2O_6]$ (wollastonite, enstatite, ferrosilite and aegirine).

4.6. HORNBLENDE-PLAGIOCLASE GEOTHERMOMETRY

Metadolerite dykes contain different generations of plagioclase and amphibole, which suggests that these rocks did not achieve a metamorphic state of equilibrium. Amphiboles are ideally used for evaluation of P-T conditions in the rocks. Indeed, as reported by Blundy and Holland (1990), these minerals are stable over a wide P-T range from 1-23 kbar and 400-1150 °C. Temperatures have been estimated using the amphibole-plagioclase thermometer by Blundy and Holland (1990). This thermometer is based on the Ca and Na equilibrium exchange between plagioclase and amphibole (Blundy and Holland, 1990). This geothermometer has been applied to different pairs of brown amphibole and PL1 and PL2 in equilibrium and in contact each other. The temperatures

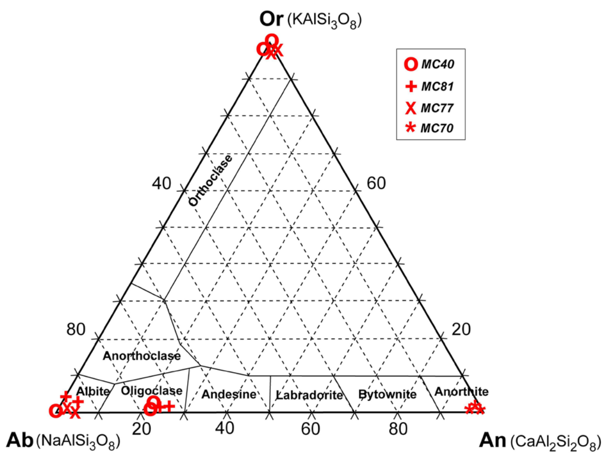

Fig. 9 - Ab-An-Or diagram showing the composition of plagioclase of metadolerite dykes.

and the pressures calculated for the M1 event (ocean-floor hydrothermal metamorphism) on the basis of brown amphibole-plagioclase pairs (Hammarstrom and Zen, 1986; Hollister et al., 1987; Johnson and Rutherford, 1989; Blundy and Holland, 1990; Holland and Blundy, 1994) range between 395° and 883 °C and 2.0-9.6 kbar (average 6.01 kbar), respectively. The P-T values estimate are reported in Tab. 5.

4.7. PHASE EQUILIBRIA AND PT PSEUDO-SECTION COMPUTATION

Pseudo-sections identify the stability of different mineralogical associations as a function of pressure and temperature fields. Pseudo-section modelling is one of

Tab. 3 - Representative chemical analyses of plagioclase (values in wt%). N.d. = Not detected.

Sample	MC81	MC81	MC77	MC77	MC77	MC81	MC81	MC77
Oxides (wt%)								
SiO_2	61.00	67.26	62.07	65.99	44.00	44.26	43.9	44.34
TiO_2	n.d	0.09	n.d	n.d	n.d	0.07	n.d	0.10
Al_2O_3	22.00	18.80	17.40	18.69	36.00	35.80	36.40	35.69
FeO	0.62	0.24	0.64	1.24	0.07	0.24	0.14	0.24
MnO	n.d	0.10	0.20	0.09	n.d	0.10	0.20	0.06
MgO	0.35	0.01	n.d	0.10	n.d	n.d	n.d	0.10
CaO	4.85	0.27	n.d	0.39	19	19.27	18.9	20.90
Na_2O	10.00	11.42	0.26	11.11	0.28	0.22	0.16	0.11
K_2O	0.02	0.03	17.04	0.09	0.05	0.03	0.04	0.07
Cr_2O_3	n.d	n.d	n.d	n.d	n.d	n.d	n.d	n.d
total	98.84	98.23	97.61	97.71	98.84	98.23	97.61	97.71
Structural formula								
Si	2.80	3.00	2.98	2.97	2.04	2.05	2.03	2.03
Ti	0.00	0.00	0.00	0.00	0.00	0.00	0.00	0.00
Al	1.13	0.99	0.98	0.99	1.97	1.95	1.99	1.92
Fe_{tot}	0.02	0.01	0.03	0.05	0.00	0.01	0.01	0.01
Mn	0.00	0.00	0.01	0.00	0.00	0.00	0.01	0.00
Mg	0.02	0.00	0.00	0.01	0.00	0.00	0.00	0.01
Ca	0.23	0.01	0.00	0.02	0.94	0.95	0.94	1.02
Na	0.85	0.99	0.02	0.97	0.03	0.02	0.01	0.01
K	0.00	0.00	1.04	0.01	0.00	0.00	0.00	0.00
Cr	0.00	0.00	0.00	0.00	0.00	0.00	0.00	0.00
Albite	0.78	0.99	0.02	0.98	0.03	0.02	0.02	0.01
Orthoclase	0.00	0.00	0.98	0.01	0.00	0.00	0.00	0.00
Anorthite	0.22	0.01	0.00	0.02	0.97	0.98	0.98	0.99

the most powerful methods to acquire thermobarometric information on rocks, because it provides a framework to interpret both textural information and mineral compositions in terms of P-T evolution (Stuwe, 1997; Cirrincione et al., 2008; Fiannacca et al., 2012; Ortolano et al., 2014). Na-amphibole and Na-pyroxene have an important role in the characterization of metamorphic conditions and are used as index minerals in the blueschist facies, to obtain estimates of pressure and temperature in the metadolerite dykes. The chemical system is represented by the Na_2O, CaO, K_2O, FeO, MgO, Al_2O_3, SiO_2, H_2O (NCKFMASH). The obtained pseudosections provided the compositions of mineral assemblages over the P-T range (3000-20000 bar and 250-600 °C for the studied rocks). SiO_2 is assumed to be in excess, as well as H_2O, that is likely considered to be the only fluid phase, due to the fact that quartz and several major hydrous phases (Chl, Ep and Amph) form part of all metamorphic stages. The NCKFMASH P-T pseudo-section calculated for sample MC77 is presented in figure 10. The minerals abbreviations and the reactions are reported in Appendix IV. The presence of Na-Amphibole can be explained by the reaction (30): Feldspar group (FSP)+omphacite (OMP)+chlorite (CHL4)+paragonite (PG)+glaucophane (GLN)+H_2O=Feldspar group (FSP)+omphacite (OMP)+ chlorite (CHL4)+paragonite (PG)+H_2O. The pressure conditions necessary for the mineralogical assemblage are approximately between 8 and 12 kbar. Pumpellyite + chlorite assemblages suggest values of pressure less than 6 kbar and temperatures below 250-300° C, constrained by the reaction (2): Feldspar group (FSP)+omphacite (OMP)+chlorite (CHL 4)+amphibole (AMP)+pumpellyite (PMP2)+paragonite (PG)+H_2O=Feldspar group (FSP)+ omphacite (OMP)+ chlorite (CHL4)+amphibole (AMP) +paragonite (PG)+ H_2O. This reaction corresponds to the transition between blueschist facies and greenschists facies.

5. DISCUSSION AND CONCLUDING REMARKS

The metadolerite dykes from the Frido Unit (southern Apennines) crosscutting serpentinite rocks are an important geological marker to understand the

Tab. 4 - Representative chemical analyses of clinopyroxene (values in wt%). N.d. = Not detected

Sample	MC77	MC77	MC77	MC77	MC77	MC77	MC77	MC77	MC70	MC70	MC70	MC70
Oxides (wt%)												
SiO_2	51.33	53.42	52.50	52.08	51.52	50.25	53.23	52.89	53.51	53.65	52.87	51.46
TiO_2	1.04	0.54	0.75	0.84	0.93	1.71	0.32	0.51	0.01	0.02	0.17	0.19
Al_2O_3	3.85	2.63	3.10	3.07	4.39	4.37	1.84	1.13	3.98	4.04	2.03	5.81
Cr_2O_3	0.03	0.39	0.12	0.01	0.16	0.03	n.d	n.d	n.d	0.01	n.d	0.01
FeO	8.02	6.05	6.09	7.78	6.15	9.04	12.57	11.94	9.04	8.95	13.69	10.73
MnO	0.23	0.15	0.17	0.32	0.14	0.29	0.33	0.38	0.30	0.27	0.63	0.46
MgO	13.90	17.53	16.30	14.13	15.58	13.43	10.54	12.19	10.71	10.51	8.77	10.79
CaO	20.98	19.81	20.93	21.20	21.01	20.46	19.69	21.34	11.31	22.73	23.20	19.88
Na_2O	1.02	0.41	0.47	0.86	0.47	0.88	2.31	0.74	1.55	1.46	0.55	1.25
K_2O	n.d	0.01	0.01	n.d	0.01	n.d	n.d	n.d	n.d	n.d	n.d	0.01
total	100.40	100.95	99.98	100.30	100.35	100.46	100.84	101.13	101.41	101.65	101.91	100.58
Structural formula												
Si	1.89	1.93	1.93	1.88	1.87	1.93	1.99	1.97	1.97	1.96	1.98	1.91
Al	0.10	0.07	0.07	0.11	0.13	0.07	0.00	0.02	0.03	0.03	0.02	0.09
Al	0.07	0.05	0.05	0.07	0.06	0.06	0.08	0.03	0.14	0.14	0.07	0.16
Fe^{3+}	0.07	0.01	0.01	0.02	0.06	0.04	0.11	0.04	0.07	0.00	0.00	0.00
Cr	0.00	0.01	0.01	0.00	0.00	0.00	0.00	0.00	0.00	0.00	0.00	0.00
Ti	0.03	0.01	0.01	0.03	0.05	0.02	0.01	0.01	0.00	0.00	0.00	0.00
Fe^{2+}	0.20	0.17	0.17	0.17	0.22	0.19	0.27	0.34	0.27	0.27	0.43	0.33
Mn	0.00	0.00	0.00	0.00	0.01	0.01	0.01	0.01	0.01	0.01	0.02	0.01
Mg	0.76	0.94	0.94	0.85	0.74	0.78	0.59	0.67	0.58	0.57	0.49	0.59
Ca	0.83	0.76	0.77	0.82	0.81	0.84	0.79	0.85	0.87	0.89	0.93	0.79
Na	0.07	0.03	0.03	0.03	0.06	0.06	0.17	0.05	0.11	0.10	0.04	0.09
K	0.00	0.00	0.00	0.00	0.00	0.00	0.00	0.00	0.00	0.00	0.00	0.00
Total	4.023	4.004	4.004	4.007	4.019	4.014	4.035	4.011	4.002	3.997	3.989	4.00
End member												
Wo	43.20	39.79	42.43	43.51	43.38	42.63	40.58	40.58	47.16	48.15	48.72	43.31
En	39.81	48.99	45.98	40.36	44.76	38.94	30.23	30.23	31.50	30.98	25.63	32.71
Fs	13.18	9.72	9.86	12.94	10.12	15.11	20.57	20.57	15.41	15.27	23.55	19.03
Aeg	3.80	1.49	1.72	3.18	1.74	3.31	8.61	8.61	5.93	5.59	2.10	4.94

metamorphic evolution of the Liguride accretionary wedge. The metadolerite dykes show a wide range of igneous texture, as intersertal/integranular to blasto-ophitic. Metadolerite rocks with mylonitic and cataclastic textures occur in the deformed domains and often the structure have been oblitered.

The serpentinized peridotite can be referred to the Jurassic Tethyan Ocean and could be considerated as the mantle portions exposed on Tethyan seafloor. Some authors (Bonatti, 1976; Mével, 1988; Cannat et al., 1997; Sansone et al., 2011) interpreted these rocks as typical of the oceanic crust generated in the slow - ultraslow spreading setting as the Atlantic. This observation is supported by the presence of the metadolerite dykes within serpentinites (Sansone et al., 2011) and it is similar to what is observed in the oceanic crustal along the Mid-Atlantic Ridge. Ophiolitic rocks underwent HP/LT orogenic metamorphism in the Liguride accretionary wedge during subduction of the western Tethys oceanic lithosphere, which produced a mineral assemblage typical of the blueschist facies conditions (Sansone et al., 2011). Amphibole and plagioclase are the main minerals in the metadolerite dykes. Based on the petrographic and electron microprobe analysis, amphibole generations testify variations of metamorphic conditions. A P-T path for the metadolerite dykes is illustrated in figure 11.

The metamorphic evolution of the metadolerite dykes records two main events:

Tab. 5 - Pressure and Temperatures values of Br-Amphibole and Plagioclase PAIRS.

Sample	MC81	MC81	MC77	MC70	MC70
Oxides (wt%)					
SiO_2	44.72	48.57	42.40	39.84	42.37
TiO_2	1.54	1.24	3.50	0.04	2.94
Al_2O_3	11.10	7.80	10.71	14.59	12.03
FeO*	12.86	11.44	19.28	29.33	15.66
MgO	0.26	0.30	0.31	0.66	0.21
MnO	14.07	16.16	9.75	3.93	11.78
CaO	10.93	10.77	10.52	8.80	10.98
Na_2O	3.16	2.52	3.18	3.35	3.73
K_2O	0.28	0.23	0.43	0.13	0.07
XAb	0.780	0.990	0.980	0.960	0.200
X An	0.220	0.010	0.020	0.100	0.970
P (kbar) [(a)]	5.9	3.1	5.8	9.1	6.8
P (kbar) [(b)]	5.8	2.5	5.7	9.6	6.8
P (kbar) [(c)]	4.5	2.0	4.4	7.3	5.2
P (kbar) [(d)]	5.9	3.1	5.8	9.1	6.8
T °C [(e)]	471.3	403.6	600.2	656.6	883.2
T °C [(f)]	470.1	398.6	600.1	659.8	883.2
T °C [(g)]	453.4	394.6	599.5	644.8	863.3
T °C [(h)]	471.3	403.3	600.2	656.6	883.2

[a] Pressure calculated using [a] (Blundy and Holland, 1990) [b] (Hammarstrom and Zen, 1986; Hollister et al., 1987); [d] (Johnson and Rutherford, 1989) [e] Temperature calculated using (Blundy and Holland, 1990) and considering [a]. [f] Temperature calculated using (Blundy and Holland, 1990) and considering [b]. [g] Temperature calculated using (Blundy and Holland, 1990) and considering [c]. [h] Temperature calculated using (Blundy and Holland, 1990) and considering [d].

1) The M1 event (ocean-floor hydrotermal metamorphism) under greenschist to amphibolite facies conditions, P=2.0-9.6 kbar (average 6.01 kbar) and T=395-883 °C, testified by the occurrence of Ca-amphiboles. The pressure ranges suggest that the oceanic floor metamorphism was not a complete process; moreover, this event was accompanied by rodingitation and spilitization process (Sansone et al., 2011).

2) The subsequent M2 event (orogenic metamorphism) developed under HP/LT blueschist and prehnite-pumpellyite facies metamorphism during the formation of the Apennine accretionary wedge. Phase equilibrium modeling suggests the following the P-T conditions 8-12 kbar and temperature of 300-400 °C. These P-T estimates are in the blueschist facies P-T range as testified by the occurrence of Ca-Na-amphiboles and interpreted as the initial stage of the orogenic phase overprinted by an orogenic-type Na-amphibole in accordance with Laurita and Rizzo (2018).

The mineralogical changes at the greenschist-amphibolite transition can be related to reaction that consumes epidote and chlorite from the greenschist assemblage and produces anorthite component of plagioclase and tschermak component of amphibole (Spear, 1993).

The brown, the green and the blue-green amphiboles show pale green/colourless amphibole rims. Amphibolite to greenschist facies conditions related to oceanic metamorphism in the Jurassic Tethys Ocean are testified by the Ca-amphibole occurrence. Some authors (Cortesogno and Lucchetti, 1984; Mével et al., 1991; Sansone et al., 2012b) attribute the presence of brown amphibole to the magmatic or late magmatic cristallization or/and to HT-oceanic alteration and this depends on their textural features. According to some authors (e.g. Spadea, 1994; Sansone et al., 2011), the occurrence of blue amphibole indicates orogenic origin and that it crystallized during subduction and records HP-LT conditions developed in the Apennine accretionary wedge.

The metamorphic history, from the emplacement in the Jurassic western Tethys to the subsequent evolution in the Apennine accretionary wedge, is testified by pseudomorphic and coronitic textures of amphibole replacing igneous clinopyroxene.

Plagioclase in the metadolerite dykes is anorthite (PL1), oligoclase (PL2) and albite (PL3). PL1 and PL2 plagioclase developed during ocean-floor hydrothermal metamorphism, instead PL3 during orogenic metamorphism. Brown amphiboles, occurring either as individual grains and overgrowths on clinopyroxene, are rich in aluminum and titanium. Clinopyroxenes probably interacted with high-T fluids to produce the Ti-pargasite amphibole that forms coronas around clinopyroxene at the temperature of the low-pressure granulite facies. Clinopyroxenes were transformed into green Mg-hornblende amphibole through hydrothermal circulation of hot seawater-derived fluids. These amphiboles could be formed in the last stage of the magmatic differentiation as the product of the crystallization of last portions of magma and reaction with the pyroxenes at the pressure of 6 kbar.

According to Puga et al. (2002) the high temperatures values deduced for the brown amphiboles based on their TiO_2 content, which range from 1.24 to 4.16 wt%, may be appropriate for the amphiboles growth during the ocean-floor hydrothermal metamorphism.

The pristine condition promoting the formation of the brown amphiboles may include several factors: high variations of the P-T, $f O_2$ conditions and also the composition of the metamorphic fluid.

The presence of pumpellyite occurring in veins as metamorphic mineral in metadolerite dykes (unusual in the oceanic environment; Mével, 1981) together with chlorite suggests low-temperature, fluid controlled, hydrothermal reaction.

In conclusion, the metadolerite dykes have been

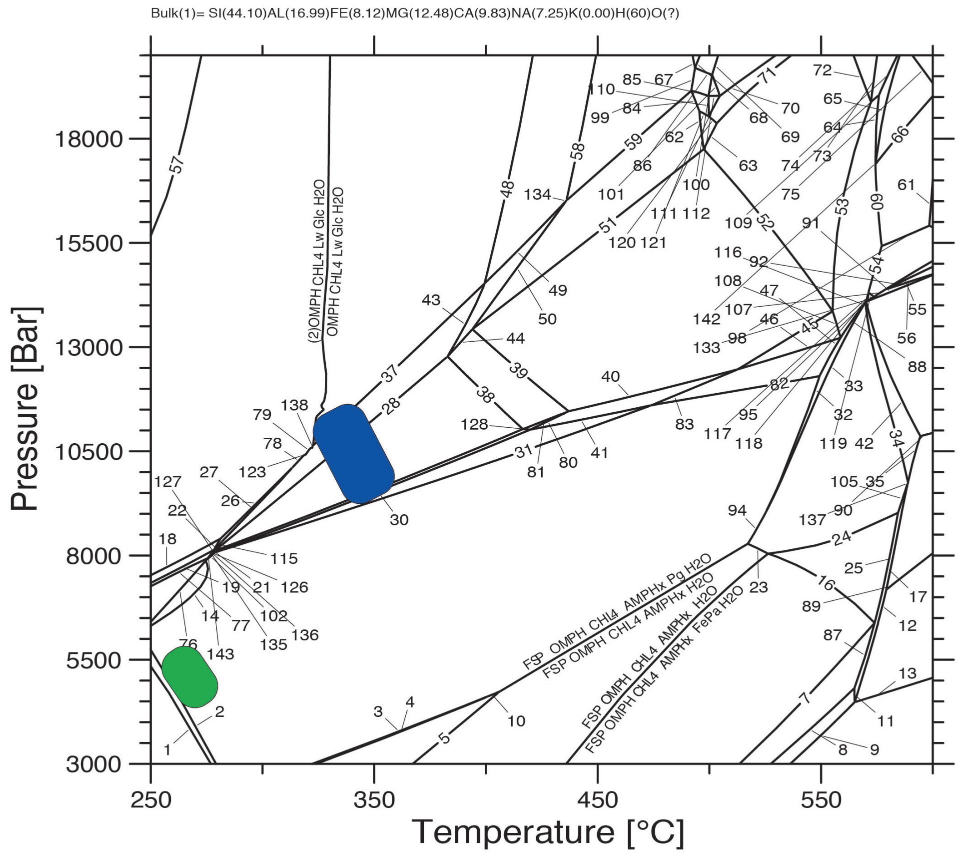

Fig. 10 - Calculated pseudo-section from MC77 sample.

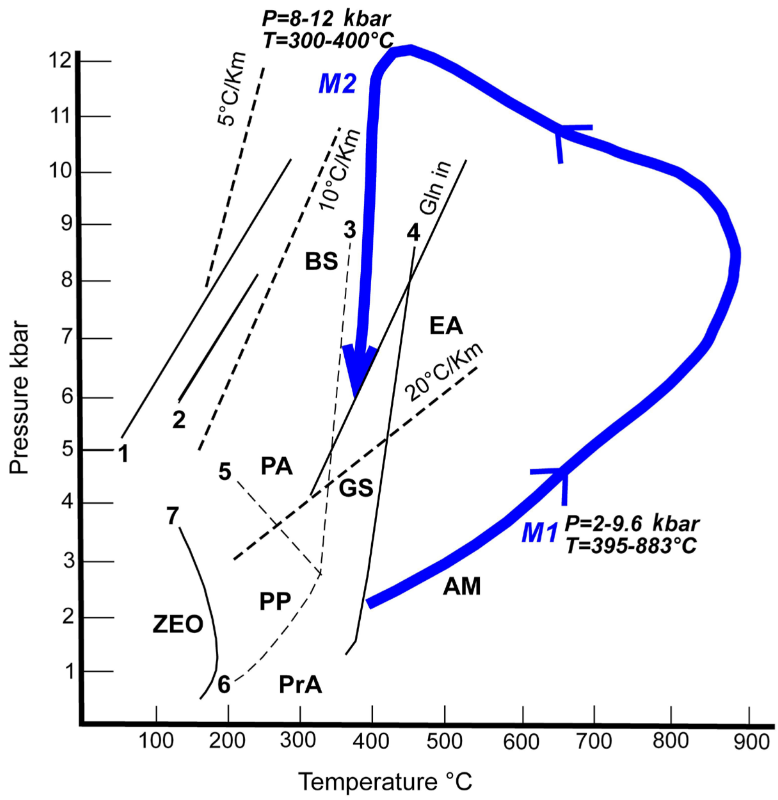

Fig. 11 - P-T path for metadolerite dykes. The lines M1 and M2 are related to the ocean-floor hydrothermal metamorphism and HP-LT metamorphism event respectively.

affected by two metamorphic events. The first (M1 event) is under amphibolite to greenschist facies conditions and using the plagioclase-brown amphibole geothermometer we have calculated the temperature values. For ocean-floor hydrothermal metamorphism the temperature ranging between 395-883 °C were estimated for the Frido Unit metadolerite dykes. Subsequently, these rocks were involved in the Apennine accretionary wedge (M2 event) testified by the occurrence of the blueschist facies and late prehnite-pumpellyite facies.

Finally the results obtained are useful for a better understanding of processes during seafloor metamorphism and for unravelling the history of the southern sector of the Apennine chain.

ACKNOWLEDGEMENTS - The authors benefited from finance support by University of Basilicata research funds.

This research was carried out in the framework of the Smart Basilicata Project, "Smart Cities and Communities and Social Innovation" (MIUR n. 84/Ric. 2012, PON 2007-2013). Many thanks to Editor in Chief (Prof. S. Milli), and two anonymous reviewers for their constructed comments and suggestions.

REFERENCES

Amodio-Morelli L., Bonardi G., Colonna V., Dietrich D., Giunta G., Ippolito F., Liguori V., Lorenzoni S., Paglionico A., Perrone V., Piccarreta G., Russo M., Scandone P., Zanettin-Lorenzoni E., Zuppetta A., 1976. L'arco Calabro-Peloritano nell'orogene Appenninico-Maghrebide. Memorie della Società Geologica Italiana 17, 1-60.

Aumento F., Loubat H., 1971. The Mid-Atlantic Ridge near 45°N: serpentinized ultramafic intrusions. Canadian Journal Earth Sciences 8, 631-663.

Barca D., Cirrincione R., De Vuono E., Fiannacca P., Ietto F., Lo Giudice A., 2010. The Triassic rift system in the northern calabrian-peloritani orogen: evidence from basaltic dyke magmatism in the San Donato unit. Periodico di Mineralogia 79, 61-72.

Berman R.G., 1988. Internally consistent thermodynamic data for minerals in the system Na_2O-K_2O-Ca-Mg-FeO-Fe_2O_3-Al_2O_3-SiO_2-TiO_2-H_2O-CO_2. Journal of Petrology 29, 445-522.

Blundy J.D., Holland T.J., 1990. Calcic amphibole equilibria and a new amphibole-plagioclase geothermometer. Contributions to Mineralogy and Petrology 104, 208-224.

Bonardi G., Amore F.O., Ciampo G., De Capoa P., Miconnét P., Perrone V., 1988. Il Complesso Liguride Auct.: Stato delle conoscenze attuali e problemi aperti sulla sua evoluzione Pre-Appenninica ed i suoi rapporti con l'Arco Calabro. Memorie della Società Geologica Italiana 41,17-35.

Bonatti E., 1968. Ultramafic rocks from the Mid-Atlantic Ridge. Nature 219, 363-264.

Bonatti E., 1976. Serpentinite protrusion from Mid-Atlantic Ridge. Earth and Planetary Science Letters 32, 107-113.

Cannat M., 1996. How thick is the magmatic crust at slow spreading oceanic crust? Journal of Geophysical Research 101, 2847-2857.

Cannat M., Lagabrielle Y., Bougault H., Casey J., De Coutures N., Dmitriev L., Fouquet Y., 1997. Ultramafic and gabbroic exposures at the Mid-Atlantic Ridge: geological mapping in the 15°N region. Tectonophysics 279, 193-213.

Cello G., Mazzoli S., 1999. Apennine tectonics in southern Italy: a review. Journal of Geodynamics 27, 191-211.

Cirrincione R., Ortolano G., Pezzino A., Punturo R., 2008. Polyorogenic multi-stage metamorphic evolution inferred via P-T pseudosections: an example from Aspromonte Massif basement rocks (Southern Calabria, Italy). Lithos 103, 466-502.

Cirrincione R., Fazio E., Fiannacca P., Ortolano G., Pezzino A., Punturo R. 2015. The Calabria-Peloritani Orogen, a composite terrane in central Mediterranean; its overall architecture and geodynamic significance for a pre-Alpine scenario around the Tethyan basin. Periodico di Mineralogia 84, 701-749.

Cortesogno L., Lucchetti G., 1984. Ocean-Floor metamorphism of metagabbros and striped amphibole (T-murlo, southern Tuscany, Italy). Neus jahrbuch fur mineralogy-abhandlungen 148, 276-300.

Dichicco M.C., Laurita S., Paternoster M., Rizzo G., Sinisi R., Mongelli G., 2015. Serpentinite carbonation for CO_2 sequestration in the southern Apennines: preliminary study. Energy Procedia 76, 477-486. doi: 10.1016/j.egypro.2015.07.888.

Dichicco M.C., De Bonis A., Mongelli G., Rizzo G., Sinisi R., 2017. μ-Raman spectroscopy and X-ray diffraction of asbestos' minerals for geo-environmental monitoring: The case of the southern Apennines natural sources. Applied Clay Science 141, 292-299. doi.org/10.1016/j.clay.2017.02.024.

Dichicco M.C., Castiñeiras P., Galindo Francisco C., González Acebrón L., Grassa F., Laurita S., Paternoster M., Rizzo G., Sinisi R., Mongelli G., 2018. Genesis of carbonate-rich veins in the serpentinites at the Calabria-Lucania boundary (southern Apennines). Rendiconti Online della Società Geologica Italiana 44, 143-149. doi.org/10.3301/ROL.2018.20.

Dichicco M.C., Paternoster M., Rizzo G., Sinisi R., 2019. Mineralogical asbestos assessment in the southern Apennines (Italy): a review. Fibers 7, 24. doi:10.3390/fib7030024.

Doglioni C., Gueguen E., Harabaglia, P., Mongelli F., 1999. On the origin of west-directed subduction zones and applications to the western Mediterranean. In: Durand B., Jolivet L., Horváth F., Séranne M. (Eds.), The Mediterranean basins: Tertiary extension within the Alpine Orogen. Geological Society of London Special Publications, 156, 541-561.

Fiannacca P., Lo Pò D., Ortolano G., Cirrincione R., Pezzino A., 2012. Thermodynamic modelling assisted by multivariate statistical image analysis as a tool for unravelling metamorphic P-T-devolution: an example from ilmenite-garnet-bearing metapelite of the Peloritani Mountains, Southern Italy. Mineralogy and Petrology 106, 151-171.

Gillis K.M., Thompson G., Kelley D.S., 1993. A view of the lower crustal component of hydrothermal systems at the

Mid-Atlantic Ridge. Journal of Geophysical Research: Solid Earth 98(B11), 19597-19619.

Gueguen E., Doglioni C., Fernandez M., 1998. On the post-25 Ma geodynamic evolution of the western Mediterranean. Tectonophysics 298, 259-269.

Hammarstrom Jane M., Zen E.-An, 1986. Aluminum in hornblende: an empirical igneous geobarometer. American Mineralogist 71, 1297-1313.

Hawthorne F.C., Oberti R., Harlow G.E., Maresch W.V., Martin R.F., Schumacher J.C., Welch M.D., 2012. Nomenclature of the amphibole supergroup. IMA Report. American Mineralogist 97, 2031-2048.

Holland T., Blundy J., 1994. Non-ideal interactions in calcic amphiboles and their bearing on amphibole-plagioclase thermometry. Contributions to Mineralogy and Petrology 116, 433-447.

Hollister L.S., Grisom G.C., Peters E.K., Stowell H.H., Sisson V.B., 1987. Confirmation of the empirical correletion of Al in hornblende with pressure of solidification of calc-alkaline plutons, American Mineralogist 72, 231-239.

Johnson M.C., Rutherford M.J., 1989. Experimental calibration of the aluminium-in- hornblende geobarometer with application to Long Valley caldera (California) volcanic rocks. Geology 17, 837-841.

Knott S.D., 1987. The Liguride Complex of Southern Italy - a Cretaceous to Paleogene accretionary wedge. Tectonophysics 142, 217-226.

Knott S.D., 1994. Structure, kinematics and metamorphism in the Liguride Complex, Southern Apennine, Italy. Journal of Structural Geology 16, 1107-1120.

Lagabrielle Y., Cannat M., 1990. Alpine Jurassic ophiolites resemble the modern central atlantic basement. Geology 18, 319-322.

Lanzafame G., Spadea P., Tortorici L., 1979. Mesozoic ophiolites of northern Calabria and Lucanian Apennine (Southern Italy). Ofioliti 4, 173-182.

Laurita S., Prosser G., Rizzo G., Langone A., Tiepolo M., Laurita A., 2014. Geochronological study of zircons from continental crust rocks in the Frido Unit (southern Apennines). International Journal of Earth Sciences (Geologische Rundschau). doi: 10.1007/s00531-014-1077-7.

Laurita S., Rizzo G., 2018. Blueschist metamorphism of metabasite dykes in the serpentinites of the Frido Unit, Pollino Massif. Rendiconti Online della Società Geologica Italiana 45, 129-135.

Lemoine M., Tricart P., Boillot G., 1987. Ultramafic and gabbroic ocean floor of the Ligurian Tethys (Alps, Corsica, Apennines): in search of genetic model. Geology 15, 622-625.

Locock A.J., 2014. An excel spreadsheet to classify chemical analyses of amphiboles following the IMA 2012 recommendations. Journal Computers & Geosciences 62, 1-11.

Magde L.S., Barclay A.H., Toomey D.R., Detrick R.S., Collins J.A., 2000. Crustal magma plumbing within a segment of the Mid-Atlantic Ridge, 35°N. Earth and Planetary Science Letters 175, 55-67.

Mével C., 1981. Occurrence of pumpellyite in hydrothermally altered basalts from the Vema fracture zone (Mid-Atlantic Ridge). Contributions to Mineralogy and Petrology 76, 386-393.

Mével C., 1987. Evolution of oceanic gabbros from DSDP Leg 82: influence of the fluid phase on metamorphic crystallizations. Earth and Planetary Science Letters 83, 67-79.

Mével C., 1988. Metamorphism of oceanic layer 3, Gorringe Bank, eastern Atlantic. Contributions to Mineralogy and Petrology 100, 496-509.

Mével C., Cannat M., 1991. Lithospheric stretching and hydrothermal processes in oceanic gabbros from slow-spreading ridges. In: Peters T., Nicolas A., Coleman R.J. (Eds.), Ophiolite genesis and evolution of the oceanic lithosphere. Petrology and Structural Geology 5, 293-312.

Mével C., Cannat M., Gente P., Marion E., Auzende J.M., Karson J.A., 1991. Emplacement of deep rocks on the west median valley wall of the MARK area. Tectonophysics 190, 31-53.

Miyashiro A., Shido F., Ewing M., 1969. Composition and origin of serpentines from the Mid-Atlantic Ridge near 24 and 30°N. Contributions to Mineralogy and Petrology 23, 117-127.

Monaco C., Tansi C., Tortorici L., De Francesco A., Morten L., 1991. Analisi geologico-strutturale dell'Unita` del Frido al confine calabro-lucano (Appennino Meridionale). Memorie della Società Geologica Italiana 47, 341-353.

Monaco C., Tortorici L., Morten L., Critelli S., Tansi C., 1995. Geologia del versante Nord-orientale del Massiccio del Pollino (Confine calabro lucano). Nota illustrativa sintetica alla scala 1:50.000. Bollettino della Società Geologica Italiana 114, 277-291.

Morimoto N., 1988. Nomenclature of pyroxenes. Mineralogy and Petrology 39, 55-76.

Morimoto N., 1989. Nomenclature of pyroxenes. Mineralogical Journal 14, 198-221.

Ortolano G., Visalli R., Cirrincione R., Rebay G., 2014. PT path reconstruction via unravelling of peculiar zoning pattern in atoll shaped garnets via image assisted analysis: an example from the Santa Lucia del Mela garnet micaschists (Northeastern Sicily-Italy). Periodico di Mineralogia 83, 257-297.

Puga E., Ruiz Cruz M.D., Díaz De Federico A., 2002. Polymetamorphic amphibole veins in metabasalts from the Betic ophiolitic association at Cóbdar, southeastern Spain: relics of ocean-floor metamorphism preserved through the alpine orogeny. Canadian Mineralogist 40, 67-83.

Raase P., 1974. Al and Ti contents of hornblende, indicators of pressure and temperature of regional metamorphism. Contributions to Mineralogy and Petrology 45, 231-236.

Rabain A., Cannat M., Escartín J., Pouliquen G., Deplus C., Rommevaux-Jestin C., 2001. Focussed volcanism and growth of slow spreading segment (Mid-Atlantic Ridge, 35°N). Earth and Planetary Science Letters 185, 211-224.

Rizzo G., Sansone M.T.C., Perri F., Laurita S., 2016. Mineralogy and petrology of the metasedimentary rocks from the Frido Unit (southern Apennines, Italy). Periodico di Mineralogia 85, 153-168.

Robinson P., Spear F.S., Schumacher J.C., Laird J., Klein K., Evans

B.W., Doolan B.L., 1982. Phase relations of metamorphic amphiboles: natural occurrences and theory. Reviews in Mineralogy 9B, 2-11.

Sansone M.T.C., Rizzo G., 2009. Rodingites dikes: Metasomatism and metamorphism in the Frido Unit (Southern Apennines). Geochimica et Cosmochimica Acta Abstract 73, A1154. Conference: 19th Annual VM Goldschmidt Conference Davos, Switzerland 21-26 June 2009.

Sansone M.T.C., Rizzo G., Mongelli G., 2011. Petrochemical characterization of mafic rocks from the Ligurian ophiolites, southern Apennines. International Geology Review 53, 130-156. doi: 10.1080/00206810902954993.

Sansone M.T.C., Rizzo G., 2012. Pumpellyite veins in the metadolerite of the Frido Unit (Southern Apennines, Italy). Periodico di Mineralogia 81, 75-92. doi: 10.2451/2012PM005.

Sansone M.T.C., Prosser G., Rizzo G., Tartarotti P., 2012a. Spinel peridotites of the Frido unit ophiolites (southern Apennines Italy): evidence for oceanic evolution. Periodico di Mineralogia 81, 35-59. doi:10.2451/2012PM0003.

Sansone M.T.C., Tartarotti P., Prosser G., Rizzo G., 2012b. From ocean to subduction: the polyphase metamorphic evolution of the Frido unit metadolerite dykes (southern Apennine, Italy). In: Zucali M., Spalla M.I., Gosso G. (Eds.), Multiscale structural analysis devoted to the reconstruction of tectonic trajectories in active margins. Journal of the Virtual Explorer 41, paper 3. doi: 103809/jvirtex.2011.00289.

Scrocca D., 2010. Southern Apennines: structural setting and tectonic evolution. In: Beltrando M., Peccerillo A., Mattei M., Conticelli S., Doglioni C. (Eds.), The geology of Italy: tectonics and life along plate margins. Journal of the Virtual Explorer 36, paper 14. doi: 10.3809/jvirtex.2010.00225.

Siivola J., Schmid R., 2007. List of mineral abbreviations. Recommendations by the IUGS Subcommission on the Systematics of Metamorphic Rocks. Paper 12. Web version 01.02.07.

Spadea P., 1976. I carbonati nelle rocce metacalcaree della Formazione del Frido della Lucania. Ofioliti 1, 431-456.

Spadea P., 1982. Continental crust rock associated with ophiolites in Lucanian Apennine (Southern Italy). Ofioliti 7, 501-522.

Spadea P., 1994. Calabria-Lucania ophiolites. Bollettino di Geofisica Teorica ed Applicata 36, 271-281.

Spear F.S., 1993. Metamorphic phase equilibria and pressure-temperature-time paths. Mineralogical Society of America, Washington, D.C., pp. 799.

Stakes D., Vanko D.A., 1986. Multistage hydrothermal alteration of gabbroic rocks from the failed Mathematician Ridge. Earth and Planetary Science Letters 79, 75-92.

Stuwe K., 1997. Effective bulk composition changes due to cooling: a model predicting complexities in retrograde reaction textures. Contributions to Mineralogy and Petrology 129, 43-52.

Tortorici L., Catalano S., Monaco C., 2009. Ophiolite-bearing mélanges in southern Italy. Geological Journal 44, 153-166.

Vanko D.A., 1986. High-chlorine amphiboles from oceanic rocks: product of highly saline hydrothermal fluids. American Mineralogist 71, 51-59.

Vezzani L., 1970. Le ofioliti della zona tra Castelluccio Inferiore e S. Severino Lucano (Potenza). Accademia Gioenia di Scienze Naturali in Catania 7, 1-49.

Vitale S., Fedele L., Tramparulo F., Ciarcia S., Mazzoli S., Novellino A., 2013. Structural and petrological analyses of the Frido unit (southern Italy): new insights into the early tectonic evolution of the southern Apennines - Calabrian arc system. Lithos 168, 219-235.

Whitney D.L., Bernard W. E., 2010. Abbreviations for names of rock-forming minerals. 677 American Mineralogist 95, 185-187.